Journal of Power Sources 183 (2008) 586–589

Contents lists available at ScienceDirect

Journal of Power Sources

journal homepage: www.elsevier.com/locate/jpowsour

Short communication

Nano-structured (La, Sr)(Co, Fe)O_3 + YSZ composite cathodes for intermediate temperature solid oxide fuel cells

Jing Chen [a], Fengli Liang [a], Lina Liu [a], Sanping Jiang [b], Bo Chi [a], Jian Pu [a], Jian Li [a,*]

[a] School of Materials Science and Engineering, State Key Laboratory of Material Processing and Die & Mould Technology, Huazhong University of Science and Technology, 1037 LuoYu Road, Wuhan, Hubei 430074, PR China
[b] School of Mechanical and Aerospace Engineering, Nanyang Technological University, Singapore 639798, Singapore

ARTICLE INFO

Article history:
Received 18 April 2008
Received in revised form 20 May 2008
Accepted 20 May 2008
Available online 8 June 2008

Keywords:
LSCF
Composite cathode
IT-SOFC
Nano-structured
Wet impregnation

ABSTRACT

A nano-structured $La_{0.8}Sr_{0.2}Co_{0.5}Fe_{0.5}O_3$ + Y_2O_3 doped ZrO_2 (LSCF + YSZ) composite cathode was prepared by impregnation of a LSCF-containing solution into porous YSZ structure presintered on the YSZ electrolyte. The result shows that the LSCF phase was formed at 700 °C, forming a nano-structured, effective and functional LSCF + YSZ composite cathode that not only produces high triple phase boundaries for the O_2 reduction reaction, but also provides a structurally stable interface between the LSCF and YSZ. The electrode polarization resistance for the O_2 reduction reaction is from 0.539 to 0.047 Ω cm^2 between 600 and 750 °C, indicating the promising potential the LSCF + YSZ as a high performance cathode for intermediate temperature solid oxide fuel cells.

1. Introduction

A solid oxide fuel cell (SOFC) consists of an anode, an electrolyte and a cathode. In thin electrolyte film SOFCs, the overall performance loss is dominated by the polarization on the cathode [1] due to the high activation energy and slow reaction kinetics for the O_2 reduction reaction; consequently, worldwide interests have been stimulated on development of the cathode, especially for the intermediate temperature SOFC (IT-SOFC).

(La, Sr)MnO_3 + Y_2O_3 doped ZrO_2 (LSM + YSZ) composite has been widely used as SOFC cathodes because of its high electrochemical activity and stability in the high temperature SOFCs; however, the electrocatalytic activity of LSM-based cathodes decreases significantly with SOFC operating temperature owing to the extremely low oxygen ion conductivity of LSM materials (~10^{-7} S cm^{-1} at 900 °C [2]). Mixed ionic and electronic conducting (MIEC) oxides, such as (La, Sr)(Co, Fe)O_3 (LSCF), possess a much higher oxygen ion conductivity (~0.18 S cm^{-1} at 900 °C [3]) and are known to be highly active for the O_2 reduction reaction in IT-SOFCs [4,5].

Unfortunately, LSCF electrodes likely react with the YSZ electrolyte to form resistive phases at temperatures higher than 900 °C [6,7] and are thermally incompatible to YSZ electrolyte, with a thermal expansion coefficient (TEC) in between 14.5×10^{-6} and 20.7×10^{-6} K^{-1} [8,9]; a Gd-doped CeO_2 (GDC) is often used as an interlayer if an LSCF cathode is considered in combination with an YSZ electrolyte [10].

In the present study, a nano-structured LSCF + YSZ composite cathode was prepared by wet impregnation of LSCF phase into presintered YSZ porous structure at a lower temperature [11], thus the commonly used high temperature sintering in cell fabrication was avoided and the adverse interfacial reaction between LSCF and YSZ was prevented. Since the prepared LSCF was in the form of nano-sized particles inside YSZ porous structure, TEC mismatch between LSCF and YSZ was alleviated.

2. Experimental

The YSZ electrolyte substrates were prepared by sintering die-pressed disks of 8%mol YSZ powder (Tosoh, Japan) at 1500 °C for 4 h in air, followed by mechanical polishing. The substrate disks were 21 mm in diameter and 1.2 mm in thickness. To establish an YSZ porous layer on the dense YSZ electrolyte, 26 nm YSZ slurry was prepared and applied to the YSZ electrolyte disks by screen printing, followed by sintering at 1200 °C for 1 h in air. The thickness of the porous YSZ layer was 8–10 μm and the active electrode area was 0.5 cm^2.

* Corresponding author. Tel.: +86 27 87557694; fax: +86 27 87557694.
E-mail address: plumarrow@126.com (J. Li).

0378-7753/$ – see front matter © 2008 Elsevier B.V. All rights reserved.
doi:10.1016/j.jpowsour.2008.05.082

The LSCF impregnation solution was prepared from $La(NO_3)_3{\cdot}6H_2O$, $Sr(NO_3)_2$, $Co(NO_3)_2{\cdot}6H_2O$, $Fe(NO_3)_3{\cdot}9H_2O$ (Sinopharm Chemical Reagent Co. Ltd.) and fluorocarbon surfactant, isopropyl alcohol and deionized water. Impregnation was carried out by placing the pre-sintered porous YSZ structure into the LSCF solution under ultrasonic treatment for 10 min. The impregnated samples were dried in air, and then fired at 700 °C in air for 1 h. The weight gain of the impregnated samples was recorded after firing. LSCF loading was ~0.4 mg cm^{-2} for one time impregnation and the process was repeated to increase the LSCF loading.

Pt paste was painted on the top of the cathodes as the current collector and on the reverse side of the electrolyte disk to form the counter and reference electrodes. The counter electrode was positioned symmetrically opposite to the working electrode and the reference electrode was painted as a ring at the edge of the electrolyte substrate. Pt mesh was attached to the Pt paste for measurement lead connections. Electrochemical impedance spectra were obtained at temperatures between 600 and 750 °C with an impedance/gain phase analyzer (Solartron 1260) and an electrochemical interface (Solartron 1287) at open-circuit. The data were collected in 40 min after the testing temperature was reached. The electrode interface resistance (R_E) was directly determined by the differences between the low- and high-frequency intercepts on the real impedance axis.

A PANalytical X'Pert PRO X-ray diffractometer was used to identify the phase formation of impregnated LSCF + YSZ composites. A Sirion 200 scanning electron microscope (SEM) was employed to examine the microstructure and distribution of impregnated LSCF nanoparticles.

3. Results and discussion

Fig. 1 shows the SEM micrographs of the fractured cross-section of the porous YSZ structure before and after LSCF-impregnation treatment. Prior to the impregnation, the YSZ porous layer was well sintered, forming a rigid three-dimensional network (Fig. 1a). After one LSCF-impregnation, the nano-sized particles between 40 and 70 nm (Fig. 1b) was observed on the surface of the porous YSZ structure with a loading of 0.4 mg cm^{-2}. With impregnation time increase, the LSCF loading was gradually risen, 1.1 mg cm^{-2} for three impregnations, some fine pores of the original YSZ porous structure were filled by LSCF nanoparticles, forming a continuous and porous LSCF + YSZ network (Fig. 1d).

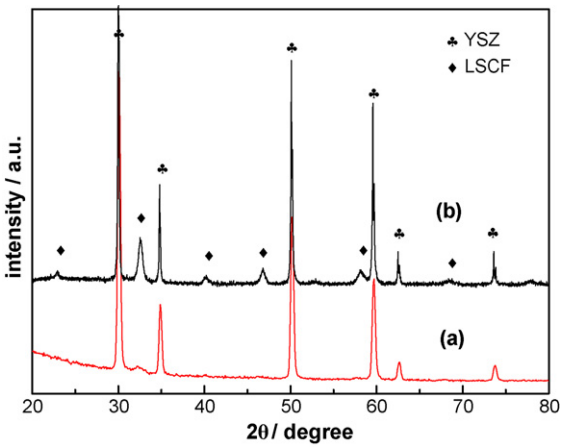

Fig. 2. XRD patterns of (a) porous YSZ structure layer and (b) nano-structured LSCF + YSZ cathode, LSCF loading ~1.1 mg cm^{-2}.

The phases of the impregnated LSCF + YSZ composite were examined by XRD, as shown in Fig. 2 for a sample impregnated three times and heat treated at 700 °C. The LSCF perovskite and YSZ structure were identified; the reaction products of LSCF and YSZ, $La_2Zr_2O_7$ and $SrZrO_3$, were not detected. This indicates

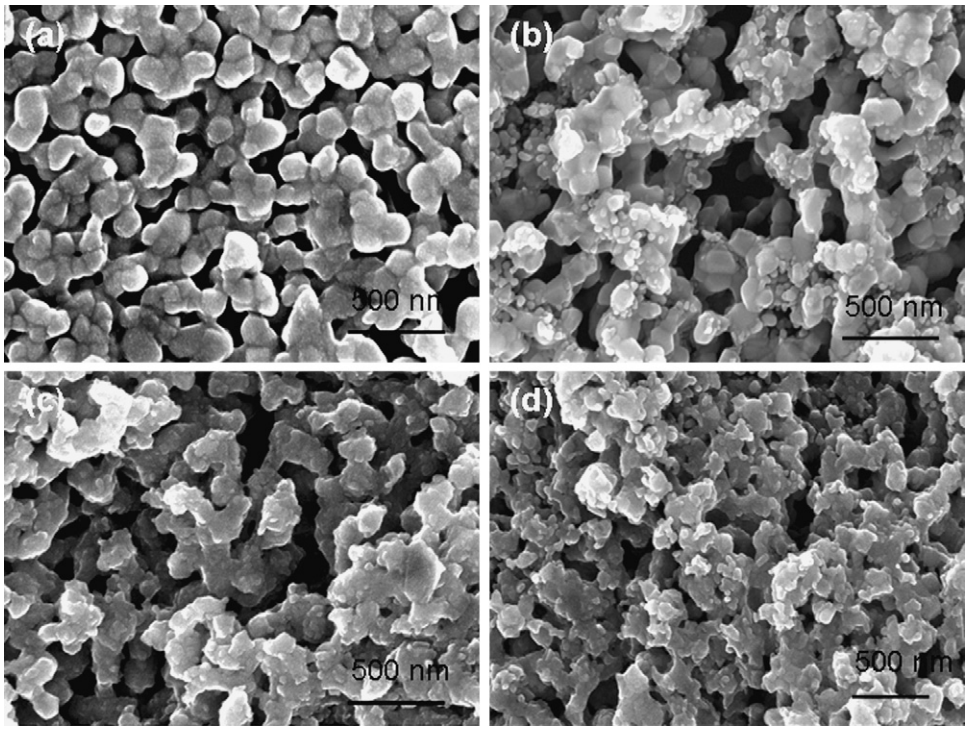

Fig. 1. SEM micrographs of fractured cross-sections of the porous YSZ structure with the LSCF impregnation treatment: (a) 0 time; (b) one time, LSCF loading ~0.4 mg cm^{-2}; (c) two times, LSCF loading ~0.8 mg cm^{-2}; (d) three times, LSCF loading ~1.1 mg cm^{-2}.

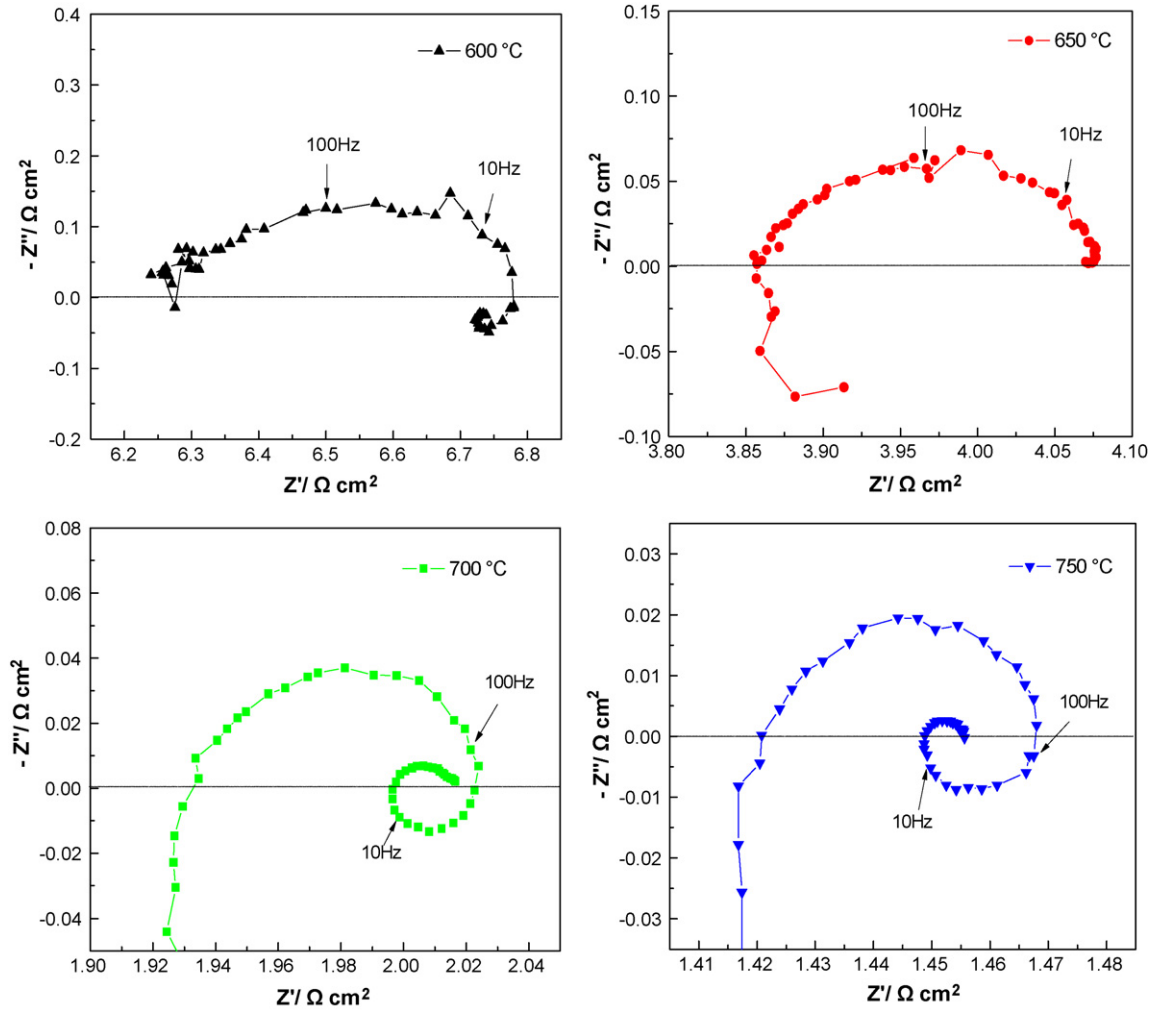

Fig. 3. Electrochemical impedance spectra of the nano-structured LSCF + YSZ composite cathode at various temperatures in air, LSCF loading ~1.1 mg cm^{-2}; scales are varied with testing temperatures.

that the formation of LSCF perovskite phase from the impregnated solution precursor can be completed at 700 °C, while the interfacial reaction between LSCF electrode and YSZ electrolyte materials was prevented at such a low formation temperature.

Fig. 3 shows the impedance spectra of a three-time impregnated LSCF + YSZ composite cathodes, measured at temperatures between 600 and 750 °C in air. The impedance responses for the O_2 reduction on nano-structured LSCF + YSZ composite cathodes are characterized by an overlapped impedance arc with a significant inductance loop at low frequencies, similar to that observed on nano-structured Pd + YSZ composite cathodes [12]. The low frequency inductance loop has been attributed to the significant adsorption/desorption process of oxygen species on the electrode surface [13]. The nano-structured LSCF + YSZ composite cathodes show an excellent electrocatalytic activity at intermediate temperatures of 600–750 °C. The electrode polarization resistance R_E for the O_2 reduction reaction in air is 0.539, 0.218, 0.089, and 0.047 Ω cm^2 at 600, 650, 700, and 750 °C, respectively. The R_E values are considered to be very low in comparison to those obtained with pure LSCF or LSCF + Gd doped CeO_2 (LSCF + GDC) composite cathodes at 700 °C, where R_E values of 0.35 Ω cm^2 [4], 0.23 Ω cm^2 [14], 0.07 Ω cm^2 [15], 0.745–0.22 Ω cm^2 [16], and 0.12–0.14 Ω cm^2 [17] were reported. Fig. 4 compares the R_E values at various temperatures obtained with the present nano-structured LSCF + YSZ composite cathode to those obtained with an A-site deficient LSCF ($La_{0.58}Sr_{0.4}Co_{0.2}Fe_{0.8}O_3$) + GDC ($Ce_{0.9}Gd_{0.1}O_2$) composite cathode [16] and a LSCF ($La_{0.6}Sr_{0.4}Co_{0.2}Fe_{0.8}O_3$) + GDC ($Ce_{0.9}Gd_{0.1}O_2$) composite cathode on YSZ electrolyte with a thin GDC interlayer [17]. Both of the LSCF + GDC composite cathodes were prepared by mixing LSCF and GDC powders. The R_E values measured with the Pt paste only is also presented in Fig. 4 to clarify the contribution made by Pt paste to the O_2 reduction reaction. It can be seen that the present nano-structured LSCF + YSZ composite cathode possesses a comparable to or better than the electrocatalytic activity of LSCF + GDC composite cathodes. The R_E with only Pt paste is the highest at all the testing temperatures, indicating that using Pt paste as the current collector for measurement does not enhance the performance of the nano-structured LSCF + YSZ composite cathode.

It is well known that the GDC electrolyte has much higher oxygen ion conductivity than the YSZ electrolyte, and the electrocatalytic activity of the LSCF + GDC composite cathode is expected to be superior to that of the LSCF + YSZ composite cathode due to its better mixed electronic and ionic conductivity. However, it is also well known that the oxygen reduction process strongly depends on the microstructure of the electrode, in particular, the particle size of the catalyst materials, since the reaction is considered to hap-

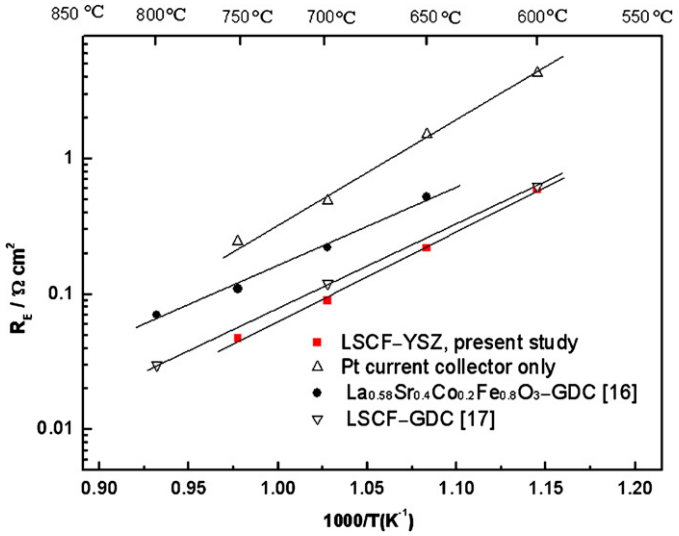

Fig. 4. Dependence of polarization resistance (R_E) in air on temperature for various electrodes: the nano-structured LSCF + YSZ composite cathode demonstrated the good performance at all testing temperatures; Pt only is not a well-performed cathode for O_2 reduction reactions.

pen at the triple phase boundaries. Such prepared nano-structured LSCF + YSZ composite cathode has two advantages over the conventional LSCF + GDC composite cathodes in microstructure: (1) the LSCF particles are nano-sized and well dispersed on top of the inner surfaces of the YSZ porous structure, generating significantly larger area of the triple phase boundary as the initiation sites for the O_2 reduction reaction; (2) the LSCF particles is form from a solution on the YSZ surfaces, an intimate contact between the catalyst LSCF particles and the YSZ surfaces is secured for a rapid ionic migration and transport. As a result, a lower polarization resistance is demonstrated for the O_2 reduction reaction.

Generally, LSCF materials are reactive at temperatures above 900 °C to form electrical resistant products and thermally mismatch with the YSZ electrolyte, which results in the introduction of an GDC interlayer between the LSCF cathode and the YSZ electrolyte or exclusion of the use of YSZ electrolyte together with LSCF catalyst materials, if conventional high temperature sintering process is adopted to fabricate the cell. However, By utilization of such developed solution impregnation method, the YSZ electrolyte materials can be selected in combination with the high performance LSCF cathode materials without an GDC interlayer.

4. Conclusions

A nano-structured LSCF + YSZ composite cathod was prepared by wet impregnation of a LSCF-containing solution into a porous YSZ structure presintered on the YSZ electrolyte. With this method, a functional LSCF + YSZ composite cathode can be formed at tempearture as low as 700 °C; nano-sized LSCF particles are well dispersed in the YSZ porous structure, significantly increasing the triple phase boundaries and generating intimate contact between the LSCF catalyst particles and the YSZ electrolyte. Consequently, a lower than usual polarization resistance for O_2 reduction reactions, such as 0.089 Ω cm^2 at 700 °C, was achieved; and the material combination of the YSZ electrolyte and the high performance LSCF catalyst for IT-SOFCs is made possible.

Acknowledgements

This research was financially supported by NSFC under Contract No. 50571038 and the “863” Project 2006AA05Z148. SEM and XRD were assisted by Analytical and Testing Center of Huazhong University of Science and Technology.

References

[1] E. Ivers-Tiffee, A. Weber, D. Herbstritt, J. Eur. Ceram. Soc. 21 (2001) 1805.
[2] I. Yasuda, K. Ogasawara, M. Hishinuma, T. Kawada, M. Dokiya, Solid State Ionics 86 (8) (1996) 1197.
[3] Y. Teraoka, T. Nobunaga, K. Okamoto, N. Miura, N. Yamazoe, Solid State Ionics 48 (1991) 207.
[4] S.P. Jiang, Solid State Ionics 146 (2002) 1.
[5] A. Esquirol, N.P. Brandon, J.A. Kilner, M. Mogensen, J. Electrochem. Soc. 151 (2004) A1847.
[6] L. Kindermann, D. Das, H. Nickel, Solid State Ionics 89 (1996) 215.
[7] H.Y. Tu, Y. Takeda, N. Imanishi, O. Yamamoto, Solid State Ionics 117 (1999) 277.
[8] L.W. Tai, M.M. Nasrallah, H.U. Anderson, D.M. Sparlin, S.R. Sehlin, Solid State Ionics 76 (1995) 259.
[9] A. Petric, P. Huang, F. Tietz, Solid State Ionics 135 (2000) 719.
[10] A. Mai, V. Haanappel, F. Tietz, D. Stöver, Solid State Ionics 177 (2006) 2103.
[11] S.P. Jiang, Mater. Sci. Eng. A: Struct. Mater. Properties Microstruct. Process. 418 (2006) 199.
[12] F.L. Liang, J. Chen, J.L. Cheng, S.P. Jiang, T.M. He, J. Pu, J. Li, Electrochem. Commun. 10 (2008) 42.
[13] L. Benea, P.L. Bonora, A. Borello, S. Martelli, F. Wenger, P. Ponthiaux, J. Galland, Solid State Ionics 151 (2002) 89.
[14] S.R. Wang, T. Kato, S. Nagata, T. Honda, T. Kaneko, N. Iwashita, M. Dokiya, Solid State Ionics 146 (2002) 203.
[15] H.J. Hwang, M.B. Ji-Woong, L.A. Seunghun, E.A. Lee, J. Power Sources 145 (2005) 243.
[16] F. Qiang, K.N. Sun, N.Q. Zhang, X.D. Zhu, S.R. Le, D.R. Zhou, J. Power Sources 168 (2007) 338.
[17] W.G. Wang, M. Mogensen, Solid State Ionics 176 (2005) 457.